X-692-71-264
PREPRINT

NASA TM X- 65621

ELECTRON ENERGY FLUX IN THE SOLAR WIND

K. W. OGILVIE
J. D. SCUDDER
M. SUGIURA

JULY 1971

GSFC
GODDARD SPACE FLIGHT CENTER
GREENBELT, MARYLAND

X-692-71-264

ELECTRON ENERGY FLUX IN THE SOLAR WIND

K. W. Ogilvie
J. D. Scudder
Laboratory for Extraterrestrial Physics
NASA Goddard Space Flight Center
Greenbelt, Maryland

and

M. Sugiura
Laboratory for Space Physics
NASA Goddard Space Flight Center
Greenbelt, Maryland

July 1971

Abstract

This paper describes studies of electrons between 25eV and 9.9keV in the solar wind. The transport of energy in the rest frame of the plasma is evaluated and shown to be parallel to the interplanetary magnetic field. The presence of electrons from solar events causes this energy flux density $E_{\parallel}$ to exceed the heat flow $H_{\parallel}$ due to thermal electrons. In one such event, the observations are shown to be consistent with the solar electron observations made at higher energies. When observations are made at a point connected to the earth's bow shock by an interplanetary field line, a comparatively large energy flux along the field towards the sun is observed, but $H_{\parallel}$ remains outwardly directed during this time interval. In either case $H_{\parallel}$ is found to be consistent with measurements made on Vela satellites by a different method. These values, less than 1×10^{-2} ergs/cm^2 / sec, are sufficiently low to require modifications to the Spitzer-Harm conductivity formula for use in solar wind theories.

Introduction

In this paper, we describe electron observations in the solar wind which cover the energy range 25eV to 9.9keV, that is, from energies characteristic of the plasma electrons to energies just below those normally observed in solar electron events. We show that transient effects can be important in determining the electron energy flux in the solar wind. We define the energy flux density along the magnetic field in the rest frame of the plasma to be $E_{\parallel}$, where the subscript indicates that the energy flows along the magnetic field. We contrast this with $H_{\parallel}$, the heat transport along the field which we assume to characterize the plasma in the absence of transient effects at higher energies. Using the constancy of the electron temperature observed both by Montgomery et al. (1968) and by the present experiment as justification, time averages of the electron observations over a period of 2 to 4 hours are used to construct the distribution function over the electron speed range 2960 km sec^{-1} to 58,900 km sec^{-1}, corresponding to the energy range 25eV to 9.9keV. Computation of the energy flux density $E_{\parallel}$ as a function of the upper limit of the velocities shows that $E_{\parallel}$ in general does not converge to a unique value.

The reason for the divergence of $E_{\parallel}$ is that the thermal electrons characteristic of the plasma, emitted continuously by the sun as a whole and making up $H_{\parallel}$, have characteristics which are not easily distinguishable from non-thermal electrons emitted from time to time by different means, since their spectra merge into one another. In addition to the transient effects of solar electrons (Lin and Anderson, 1967, Lin, 1970), which can make large contributions to $E_{\parallel}$ between ~340eV and 9.9keV, a net energy flux towards the sun is observed when the detector is situated on a magnetic field line intersecting the earth's bow shock surface.

As a result of the influence of these transient effects at the higher energies, the shape of histograms of $E_{\parallel}(E_u)$, where E_u is a fixed upper energy limit, might only partially represent the heat flux variability. The present observations indicate that for $E_u \lesssim 0.340$keV, when $E_{\parallel}(E_u) \sim H_{\parallel}$, the heat flux has values consistent with those of Montgomery (1971 a), and therefore support his conclusions regarding the plasma conductivity.

Montgomery et al. (1968) have calculated the third moments of the electron velocity distribution function in the solar wind using detailed measurements up to 1600eV from Vela satellites. Determining the energy flux density in the rest frame of the plasma, $E_{\parallel}$, they interpreted this at quiet times as the heat flux $H_{\parallel}$. The contribution of protons to the heat flux is about one thousandth of that carried by the electrons.

More recently Montgomery et. al.(1971a,b) has reported a most probable value of the heat flux $\langle H_{\parallel} \rangle \simeq 0.6\text{-}.7\text{x}10^{-2}$ergs $cm^{-2}sec^{-1}$. Such a low value is not consistent with the predictions of current solar wind theory, using the Spitzer-Harm conductivity formula (Montgomery et. al., 1971a). The measurements refer to higher bulk speeds (~300 - 325 km sec^{-1}) than those predicted by the theories (~260 km sec^{-1}). These higher bulk speeds, presumably requiring the deposition of energy in the heliocentric range 2-25 solar radii, should accompany higher heat fluxes than those presently predicted, which are already much larger than the experimental results, Hundhausen (1970) . One-fluid theories with modified conductivity which can predict $H_{\parallel}$ close to the observed values, using the observational data as a boundary condition, have been reported (Cuperman and Harten, 1970, Whang, 1971, Wolff, Brandt and Southwick, 1971). Because of the connection with the transport parameters of the plasma, measurements of $E_{\parallel}$ are of interest, especially if carried out by different methods.

Experimental

The observations described in this paper were made using the triaxial electron spectrometer on OGO-5, described elsewhere (Ogilvie, et al. 1971). Three cylindrical electrostatic analysers accepted electrons whose directions of motion fell into three cones of ten degree half angle. The axes of these cones were mutually perpendicular, and made equal angles to the normal $\hat{n}$ to the mounting face of the satellite body. The attitude control system maintained the direction of $\hat{n}$ pointing always away from the earth. The data to be discussed here were taken when the spacecraft was in the interplanetary medium close to apogee, (~24 R_e) on outward legs of its orbit. The angle between the heliocentric direction and that of $\hat{n}$ varied less than one degree per hour during these periods, so that the direction of the detectors can be considered to have been fixed relative to the earth. Every 23 seconds the analyzers simultaneously measured the energy spectrum of electrons entering at three different angles β with respect to the magnetic field. The constancy of the detector sensitivity was checked by 3 radioactive sources and intercalibration between the detectors was checked using the data itself.

Technique

The basic assumptions of our analysis are a). the axial symmetry, and b). the near time-independence, of the velocity distribution about the interplanetary magnetic field line. Thus in a polar coordinate system, with the magnetic field direction along the polar axis, the distribution function is independent of the azimuth φ and the time t. An argument in favor of such an assumption is that T_e, a statistic of this distribution, is found experimentally to be essentially constant in time and the electron anisotropy is small (~1.1 - 1.2) even when proton temperatures are highly variable, (Montgomery

et al 1968). We therefore assume that $<f(v,\beta(t),\alpha(t))>$ constructs $<f(\vec{v})>_t$, where v is the magnitude of the total velocity $\vec{v}$; $\beta(t)=\cos^{-1}(\hat{B}(t)\cdot\hat{V})$ is the angle that $\vec{v}$ makes with the field line, $\alpha(t)$ the angle between $\hat{u}$ and $\hat{v}$ as a function of time. In other words the time dependence of the measurements enter essentially through that of β, since α is almost a constant during a given measurement.

Correlation Between Electron Energy Flux Direction and the Magnetic Field Direction in the Interplanetary Medium

The energy flux vector of the plasma is the third moment of the distribution function, whose components

$$Q_j \equiv \iiint \frac{m}{2}\|v-u\|^2(v_j-u_j)f(v,\beta,\varphi,t)v^2\,dv\sin\beta\,d\beta\,d\varphi$$

$$= 2\pi\iint \frac{m}{2} w^3 w_j f'(w,\beta',\varphi',t)Jw^2\,dw\sin\beta'\,d\beta'$$

where $J \equiv \partial(v,\beta,\varphi)/\partial(w,\beta',\varphi')$ is the Jacobian of the transformation into the rest frame of the plasma, in which w,β', and φ' are the coordinates. In these equations $\vec{w} = \vec{v} - \vec{u}$, where $\vec{v}$ is the total velocity vector of the electron, u is the bulk speed, and w_j is the jth component of $\vec{w}$. Thus, w is the random velocity with respect to the rest frame of the plasma. We also define the magnitude of the energy flux vector per unit solid angle as

$$Q_\Omega(\beta',E_u) \equiv \int_{E_L}^{E_U} \frac{mw^3}{2} f'(w,\beta',t)Jw^2\,dw$$

where E_L is the energy corresponding to the lowest velocity.

$$= \int E(w)\{f'(w,\beta',t)w^2/m\}JdE(w)$$

$$\simeq \int E(w)\{f'(w,\beta',t)v^2[1-2u\cos\alpha/v+u^2/v^2]^{3/2}/m\}dE(w)$$

where $J \approx \|w\|/\|v\|$. Since $f'(w,\beta',t) \simeq f(v,\beta,t)$

$f'(w,\beta',t)v^2/m \simeq$ the measured differential flux.

We thus obtain that

$$Q_\Omega \simeq \int E(w)\text{Flux}[1 - 2u\cos\alpha/v+u^2/v^2]^{3/2}dE(w)$$

The bulk speeds used here were obtained from the MIT experiment on Explorer 35 (Binsack, private communication), since they were not obtained from the present experiment with sufficient accuracy. The units in which this flux is expressed is particles/cm^2/str/kev. It will be noted that Q_Ω is a function of the highest energy employed in the distribution determination, E_U which is the upper limit of all the above integrals; the lower limit, E_L, is, unless noted otherwise, equal to 25eV. These and all subsequent integrals were evaluated numerically by interpolating a cubical spline through the data and integrating the result. Such an interpolant injects minimal prejudice to the quadrature determination in the sense that it is the smoothest curve which interpolates all the data (Thompson, 1970), (Scudder, 1971).

Let us examine $\langle Q_\Omega \rangle$ as a function of θ. Three alternative possibilities for the energy transport are shown schematically in Figure 1. If there were no preferred direction of the energy transport with respect to the field,

$\langle Q_\Omega(\beta)\rangle$ vs β would appear as shown in the upper panel. If there were a loss cone about the field direction such a plot would resemble the middle panel. The transport of energy essentially parallel to the field without loss cone (β=0 or π) would lead to a dependence of $\langle Q_\Omega\rangle$ upon β as shown in the lower panel, (or its reflection in $\beta = \pi/2$), where the flux is constant within a cone about the direction of $\bar{B}$, (or $-\bar{B}$).

For several periods when the spacecraft was in the interplanetary medium we have plotted $\langle Q_\Omega(\beta)\rangle$ in this manner. To avoid possible interference from terrestrial effects, we have picked for our first examples times when the interplanetary field had a low probability of bow shock intersection, and two such summaries are shown in Figure 2. On the right is an example taken from a positive magnetic sector when the field was directed away from the sun and U=380 km sec^{-1}, and on the left from a "toward" or negative sector, when U=410 km sec^{-1}. The data points are averages over five degree intervals of β. Whenever the β_i of the ith detector of the triad is in the Jth angular interval, its value of $Q_\Omega(\beta_i \subset \beta_J)$ is averaged with other such determinations at subsequent times regardless of i. This technique directly exploits the assumed time independence and axial symmetry of f(w) as outlined above. Because of the variability of the field direction, more than one detector generally contributes to the average characteristic of an angular interval. All three detectors sometimes contribute to the high flux regions shown in Figure 2. If the forward cone is uniformly populated, as is indicated by a flat step on the right, the interdetector calibrations can be checked, and small corrections to the data made by normalizing with respect to one detector.

The March 8 example is from a negative magnetic sector, i.e. B field toward the sun. The upper (diamond) curve shows energy flowing away from the sun occupying a band of directions at about 120° from the magnetic field

direction, for an electron energy range of 25eV to 9.9keV. The lower curve (crosses) shows a similar graph covering the energy range 25eV to 340eV. When modified by the cos β sin β geometrical factor (see Eq. 3) this yields a small net heat conduction anti-parallel to the field, i.e. away from the sun. In the March 13 example two similar curves are presented for a time when the transient contribution to $E_{\parallel}$ was much larger and when the magnetic field direction was reversed, (note the change in vertical scale). The peak for the higher energies now occurs for angles $<50^{o}$, and there is no empty cone. At lower energies a small energy flux away from the sun is still measured.

These plots are thus consistent with energy transport at all observed energies being parallel to the field line and flowing away from the sun regardless of the average polarity of the sector structure. The minima of $\langle Q_{\Omega}(\beta)\rangle$ in the transverse direction to the field suggest the inhibition of electron energy conduction in this direction. Figure 2 shows that the time average direction of maximum $\bar{Q}$ is correlated with that of $\bar{B}_e$ where $\hat{B}_e$ is the earthward direction along an interplanetary field line. In Figure 3 we present similar evidence on a shorter time scale. Here $Q_{\Omega}(\beta(t))$ is plotted isometrically against β and time for each detector, each point being separated by a time interval of 23 secs. These examples are from outward sectors and therefore when β is near 0, $Q_{\Omega}(\beta)$ should be larger than when β is $\gtrsim 70^{o}$. We have divided the energy range E_L to E_u into two parts; E_L and E_u are 25eV and 340eV in the upper panel and 550eV and 2300eV in the lower panel. Both panels show that the detector having the smallest value of β measures the largest value of $Q(\beta)$. Thus in each case the net energy flux $E_{\parallel}$ is closely correlated with the field direction $\hat{B}$.

Similar studies are being made of the transport of energy by electrons along field lines which intersect the earth's bow shock. Figure 4 shows an example obtained during a four hour period on March 19, 1968 when OGO-E was situated at $X_{SE} \tilde{=} 13.1\ R_e, Y_{SE} \tilde{=} -12.6\ R_e, Z_{SE} \tilde{=} 13.7\ R_e$, very close to the bow shock in the dawn meridian when the interplanetary field sector was positive. Here $\langle Q_\Omega \rangle$ is plotted against β, and during this time field line intersection with the bow shock was almost certain. The crosses in Figure 4 represent Q_Ω calculated up to 210eV, and indicate a net heat flux $H_\parallel$ <u>from</u> the solar direction. The diamond-shaped points, however, represent $\langle Q_\Omega \rangle$ calculated up to 9.9keV and indicate a large energy flux from the bow shock direction <u>towards</u> the sun. Protons of energy ~5 keV have been observed upstream of the bow shock (Asbridge et al. (1968), Frank and Shope (1968) which suggest that the present phenomenon is probably associated with electron flow from the shock as has been inferred by Fredericks, Scarf and Frank, (1971). In this example, all the observed backward cone angles contribute to the reverse flow, in contrast to Figure 2, where electron flux from the sun is confined to a cone of half angle $\sim 70^\circ$. Thus electrons from the sun were somewhat better collimated than those from the bow shock.

<u>The Magnitude of Energy Flow in the Solar Wind</u>

The energy transport parallel to the magnetic field is

$$(E_\parallel) \equiv \vec{Q}.\hat{B} = 2\pi \int_0^\pi \langle Q_\Omega(\beta, E_u) \rangle \sin\beta \cos\beta \, d\beta$$

where the explicit dependence of $E_\parallel$ on E_u is noted and the axial symmetry used. If transient energy flow from the sun as well as quasi-steady heat conduction, $H_\parallel$, existed in the solar wind, $E_\parallel$ vs log E_u might look as in

Figure 5. In the upper panel the convergence of $E_{\parallel}$ below some energy E_c allows an unambiguous determination of $H_{\parallel}=E_{\parallel}(E_c)$. If transient energy flow occurs at lower energies, as in the lower two panels, $H_{\parallel}$ no longer equals $E_{\parallel}(E_c)$ but is $E_{\parallel}(E_o)$ where $E_o<E_c$. The bottom panel illustrates the case where the electrons providing the transient energy flow are associated with the earth's bow shock. The thermal electron population still provides a flux of heat away from the sun, and the population at higher energies a flux of energy directed towards the sun.

Figure 6 shows $E_{\parallel}$ vs log E_u plots for three periods of observations in the interplanetary medium, for which bow shock intersection of the threading magnetic field line is improbable. Each curve is from a different apogee on a succession of apogees in the interval March 8-13, 1968 and they are marked A, B, C on the inset diagram. The examples are successively more divergent, in the sense of Figure 6, as the day number increases. It will be seen that extrapolating the trend of the high energy parts of the curves to $E_{\parallel}=0$, indicates that the energy separating the electron heat flux $H_{\parallel}$ and the contributions to $E_{\parallel}$ due to transient electrons is about 340eV, since above this energy $E_{\parallel}$ increases rapidly with E. Also, we see that at high energies $E_{\parallel}$ increases with time, whereas the value of $H_{\parallel}(\sim E_{\parallel}(340\text{eV}))$ remains about the same within the uncertainties of our determinations, and is certainly less than 10^{-2} ergs cm^{-2} sec^{-1}.

Comparison between the present results and data of Lin and Anderson (private communication) show that the highly anisotropic flux of electrons having energies between 340eV and 9.9keV tracks that of electrons having energies greater than 22keV. The electrons observed here are thus

associated with the same solar event as those observed by Lin and Anderson and are the cause of the divergences. This conclusion is made more plausible by Figure 7, where we see points from Lin and Anderson at 26keV and from the present experiment above 890eV obtained on March 8 and 11. The present observations are joined to those of Lin by the smoothest curve, (Thompson, 1970). At 26keV, the slope of the curve is that observed over the energy range 22-45keV by Lin. Although Explorer 35 passed into the tail before our next series of interplanetary observations, the Forbush decrease after the SC continued well past the March 13th observation by OGO-E, which indicated further enhanced levels of fluxes in the non-thermal portion of the plasma distribution function causing the more divergent nature of $E_{\parallel}$.

Figure 8 shows the value of $E_{\parallel}$ plotted against log E_u for a bow-shock intersecting case. At energies below ~210eV the energy flow, the plasma heat flux, is toward the earth, but at higher energies the flow is much larger and towards the sun, away from the bow shock. The values of $\bar{H}_{\parallel} \equiv E_{\parallel}(1600)$ presented by Montgomery were obtained by making detailed measurements of $f(\bar{v})$ below E_u (+1600eV) on Vela spacecraft which were in nearly circular orbits of radius 19 R_e. These orbits were closer to the average bow shock position than the regions where the present data was obtained. Since the Vela spacecraft do not carry magnetometers, the magnetic field direction at the spacecraft was not known, and partitioning the data into sets associated with intersecting and non-intersecting field lines was approximately carried out by noting whether or not there was a significant component of heat flux coming from the earthward direction along the field. In addition, if outward streaming protons were present it was assumed that the spacecraft was on a bow shock connected field line, (Montgomery - private communication).

In view of the above discussion of transient effects due both to bow shock intersection and to solar electron production, $H_{\parallel}$ is not always easy to deduce from such measurements. It is therefore very satisfactory that the values of $H_{\parallel}$ ($\sim 4 \times 10^{-3}$ ergs cm^{-2} sec^{-1}) obtained here are in good agreement within the experimental errors of $\pm 25\%$ with those obtained by Montgomery.

Thus, the conclusions, based upon the small values of $H_{\parallel}$, drawn by Hundhausen and Montgomery (1970) are supported by the present measurements.

Conclusions

From these measurements of electron energy fluxes we conclude;

a). A detector situated on an interplanetary magnetic field line not intersecting the earth's bow shock measures a net electron energy flux away from the solar direction along the field line. The direction of this energy flux is independent of the polarity (sign) of the interplanetary field, and very strongly correlated with the instantaneous magnetic field direction at all energies up to 10 keV.

b). By making comparison between our observations and those of Lin and Anderson during a solar electron event, we conclude that the present observations extend those of Lin and Anderson to lower energies. Solar electrons are apparently emitted with energies as low as 350eV, and contribute decisively to $E_{\parallel}$ during these events.

c). When the detector was situated on a line of force of the interplanetary field which had a high probability of intersecting the earth's bow shock, it indicated a substantial energy flux at energies >210 eV, towards the sun along the field. The energy flux at energies <210 eV continued away from the sun. This suggests the possibility of the acceleration of electrons from energies characteristic of the plasma up to energies of several keV at the shock. The bulk speed of the plasma was ~600 km sec^{-1} at the time of the example given in this paper.

d). $H_{\parallel}$, the heat flux density, has been measured in four cases by calculating $E_{\parallel}$ up to an energy E_u where the effect of transient electrons becomes noticeable. The values obtained, while not of high accuracy, are certainly $<1x10^{-2}$ ergs/cm^2/sec, and thus are in agreement with the low values measured by Montgomery. The average bulk speed during these measurements were approximately 385 km sec^{-1}, except on March 19.

ACKNOWLEDGEMENTS

The authors have had many useful discussions with Dr. K. H. Schatten, and wish to thank him and Dr. R. P. Lin for comments. We wish to thank Dr. Lin for permission to use his observations in Figure 7, and Dr. Don Lind for his help in designing and calibrating the spectrometer.

FIGURE CAPTIONS

Figure 1 Schematic representation of energy flux density $\langle Q_\Omega(\beta)\rangle$ vs. β for various physical situations; A). energy flux uncorrelated with field direction; B) correlation with empty cone about field; C) energy flux filling cone about field line.

Figure 2 Plots of $\langle Q_\Omega(\beta)\rangle$, the differential contributions to the energy flux density per unit solid angle, for angular intervals of 5^o. Note that β is the angle between $\vec{v}$ and $\vec{B}$.

Figure 3 Isometric plots for each detector showing that the largest flux is detected by that detector "looking" closest to the magnetic field line, and that this condition is preserved as the magnetic field direction shifts with respect to the triad of directions of the detectors. This is interpreted as showing that the energy flux is greatest along the field direction away from the sun.

Figure 4 A plot of $\langle Q_\Omega(\beta)\rangle$ against β for a period when the interplanetary magnetic field intersects the earth's bow shock. The diamond shaped points, E_u=9.9 keV, refer to the ordinate scale on the right, the crosses, E_u=210eV, to the scale on the left.

Figure 5 This figure illustrates a possible difficulty in the evaluation of $H_{\|}$ from measurements of $E_{\|}$ up to a fixed energy E_u.

Figure 6 $E_{\|}$ as a function of Log E_u for 3 periods during a "delayed" electron event (Lin and Anderson, private communication). The crosses (pt. A in the inset) refer to a time of low solar electron flux, the squares (pt. B in the inset) refer to a time of high solar electron flux. The event is discussed further

in the text. Note how extrapolating back to $E_{\parallel}=0$ on all three curves crosses the axis between 210-340 eV.

Figure 7 Illustrating how the electron spectra of Lin and Anderson join onto those determined by the present experiment. Average differential flux values obtained on 8 March and 11 March 1968 are shown. A correction for the different solid angles of the detectors has been applied, and the steepness of the spectrum between 22 keV and 45 keV (power law index -4.4) has been used in inferring what energy most of Lin's particles had. Seventy five percent of the particles had energies between 22 and 31 keV.

Figure 8 The net energy flux $E_{\parallel}$ plotted against log E_u, the uppermost energy to which it is calculated. Values of $E_{\parallel}>0$ represent flux direction away from the sun, and values <0 represent flux toward the sun (away from the earth's bow shock) along the magnetic field line. In this example the field almost certainly intersects the earth's bow shock.

REFERENCES

Asbridge, J. R., S. J. Bame and and I. B. Strong, "Outward flow of protons from the earth's bow shock", J. Geophys. Res., 73, 5777, 1968.

Cuperman, S., and A. Harten, "The solution of one-fluid equations with modified thermal conductivity for the solar wind", Cosmic Electrodynamics, 1, 205, 1970.

Frank, L. A. and W. L. Shope, "A cinematographic display of observations of low energy proton and electron spectra in the terrestrial magnetosphere and magnetosheath and in the interplanetary medium", Trans. Am. Geophys. Union, 49, 279, 1968.

Fredricks, R. W., F. L. Scarf, L. A. Frank, "Non-thermal electrons and high frequency waves in the upstream solar wind, I, II", TRW reprint 05402-6026-7, RO-00, 1971.

Hundhausen, A. J. and M. D. Montgomery, "Heat conduction and non-steady phenomena in the solar wind", J. Geophys. Res., 76, 2236, 1971.

Hundhausen, A. J., "Composition and dynamics of the solar wind plasma", Reviews of Geophysics and Space Science, 8, 729, 1970.

Lin, R. P. and K. A. Anderson, "Electrons >40 keV and protons >500 keV of solar origin", Solar Phys., 1, 446, 1967.

Lin, R. P., "The emission and propagation of ~40 keV solar flare electrons", Solar Phys., 12, 266, 1970.

Montgomery, M. D., S. J. Bame, and A. J. Hundhausen, "Solar Wind electrons: Vela 4 measurements", J. Geophys. Res., 73, 4999, 1968.

Montgomery, M. D., S. J. Bame and J. R. Asbridge, "Solar wind electrons - average properties", abstract, Trans. Amer. Geophys. Union, 52, 336, 1971a.

Montgomery, M. D., J. R. Asbridge and S. J. Bame, "Solar wind electrons -- Vela IV average properties", to be submitted to J. Geophys. Res. 1971b.

Ogilvie, K. W., J. D. Scudder, M. Suguira, "Magnetic field and electron observations near the dawn magnetopause, J. Geophys. Res., 76, 3574, 1971.

Scudder, J. D., "Spline Quadrature, NASA-GSFC X-692-71-200, 1971.

Thompson, R. F., "Spline interpolation on a digital computer, NASA-GSFC X-692-70-261, 1970.

Whang, Y. C., "Conversion of magnetic field energy into kinetic energy in the solar wind", submitted to Astrophys. J.

Wolff, C. L., J. C. Brandt and R. G. Southwick, "A two component model of the quiet solar wind with viscosity, magnetic field and reduced heat conduction", Astrophys. J., 165, 181, 1971.

Figure 1

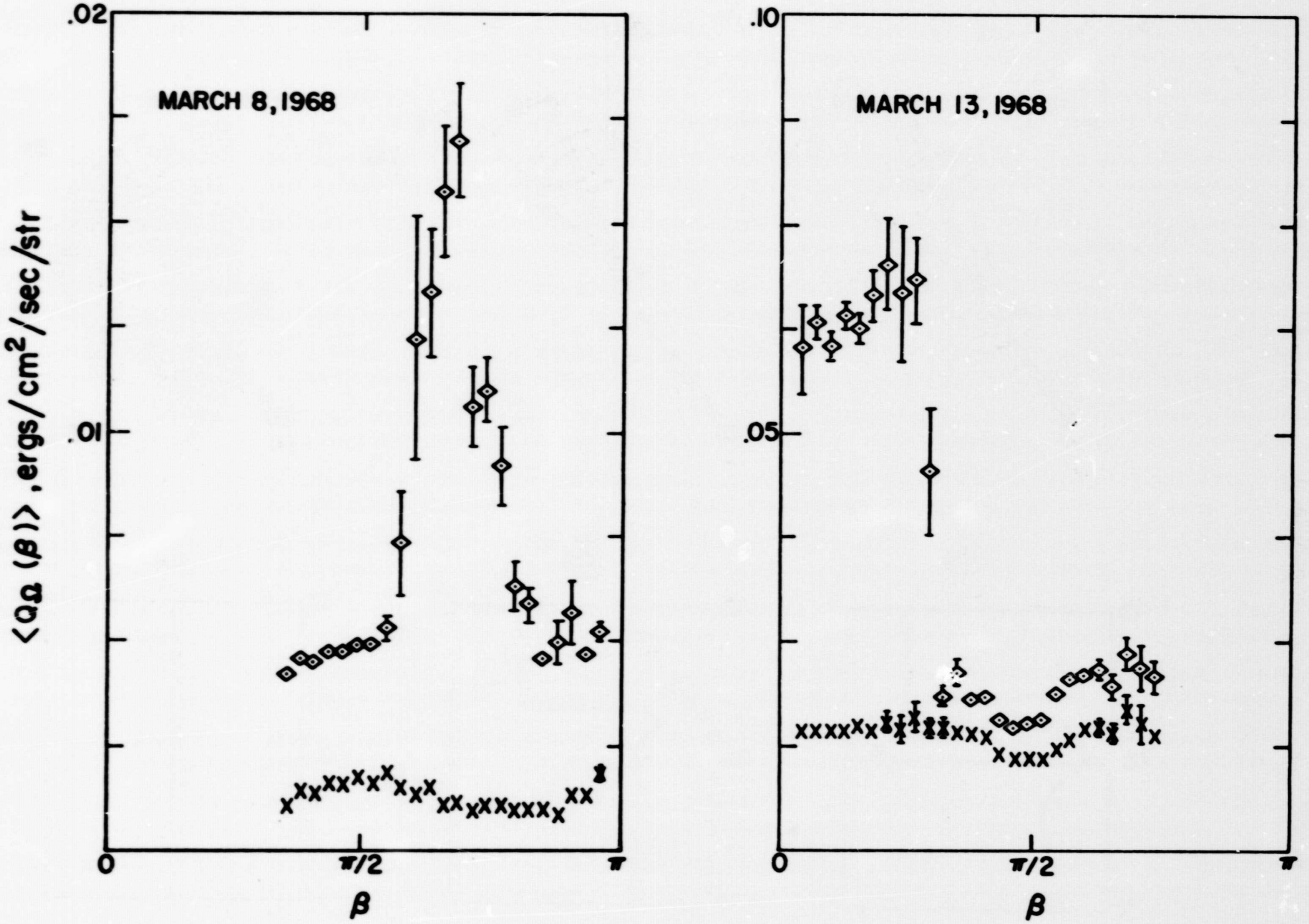
MARCH 8, 1968
MARCH 13, 1968
.02
.01
.10
.05
0
π/2
π
β
⟨Qω (β)⟩, ergs/cm²/sec/str

Figure 2

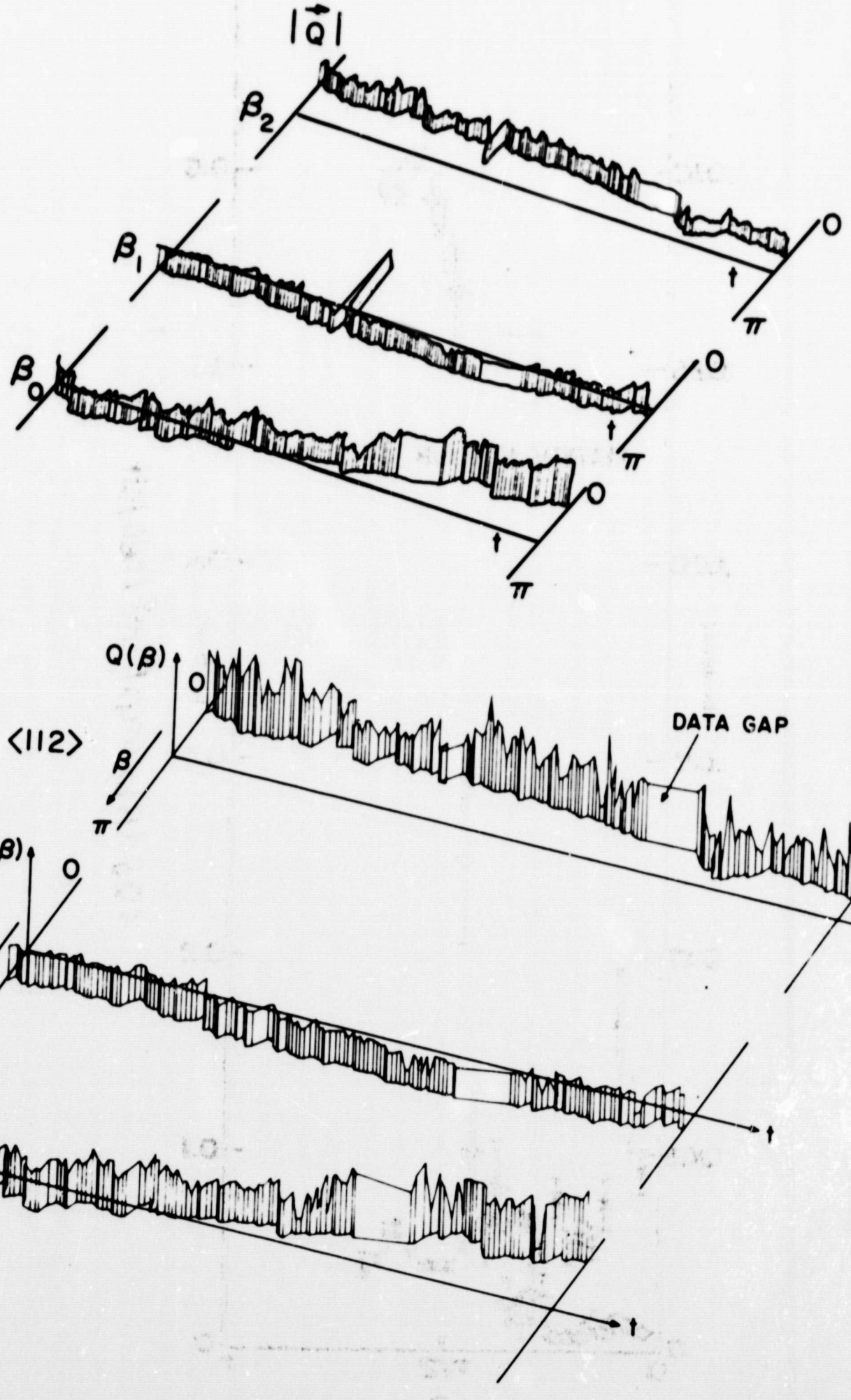

Figure 3

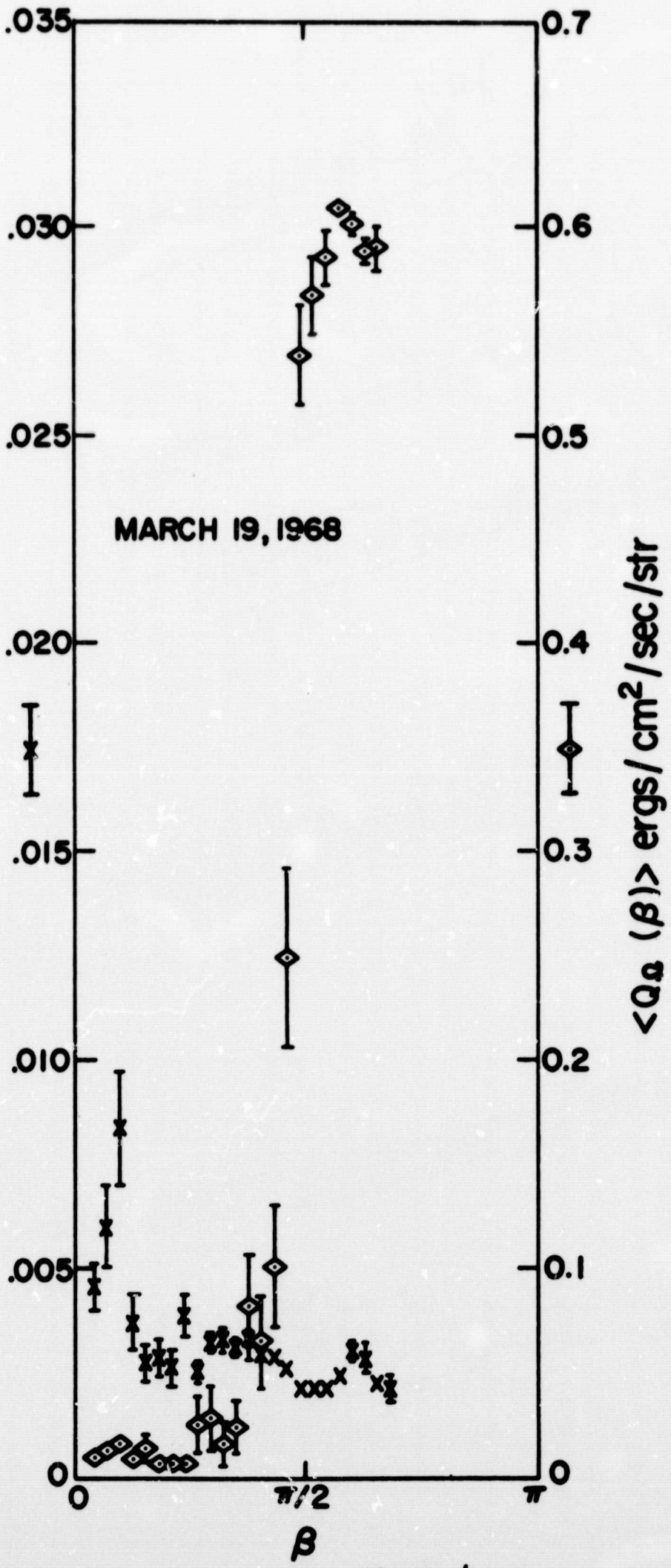
.035
.030
.025
.020
.015
.010
.005
0
0.7
0.6
0.5
0.4
0.3
0.2
0.1
0
MARCH 19, 1968
0
π/2
π
β
<Qa (β)> ergs/cm²/sec/str

Figure 4

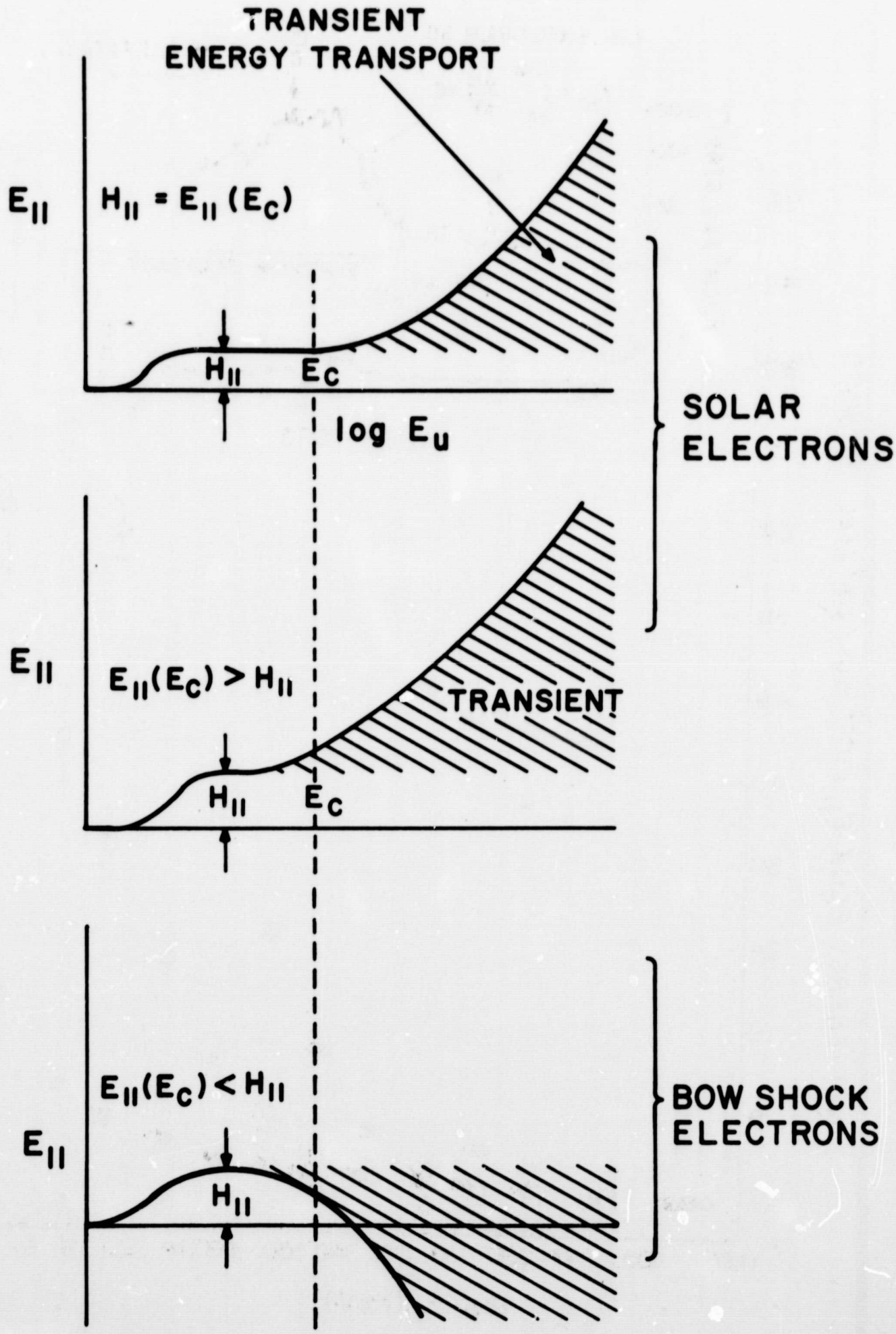
TRANSIENT
ENERGY TRANSPORT
E_{II}
$H_{II} = E_{II}(E_C)$
H_{II}
E_C
log E_u
SOLAR
ELECTRONS
E_{II}
$E_{II}(E_C) > H_{II}$
TRANSIENT
H_{II}
E_C
$E_{II}(E_C) < H_{II}$
E_{II}
H_{II}
BOW SHOCK
ELECTRONS

Figure 5

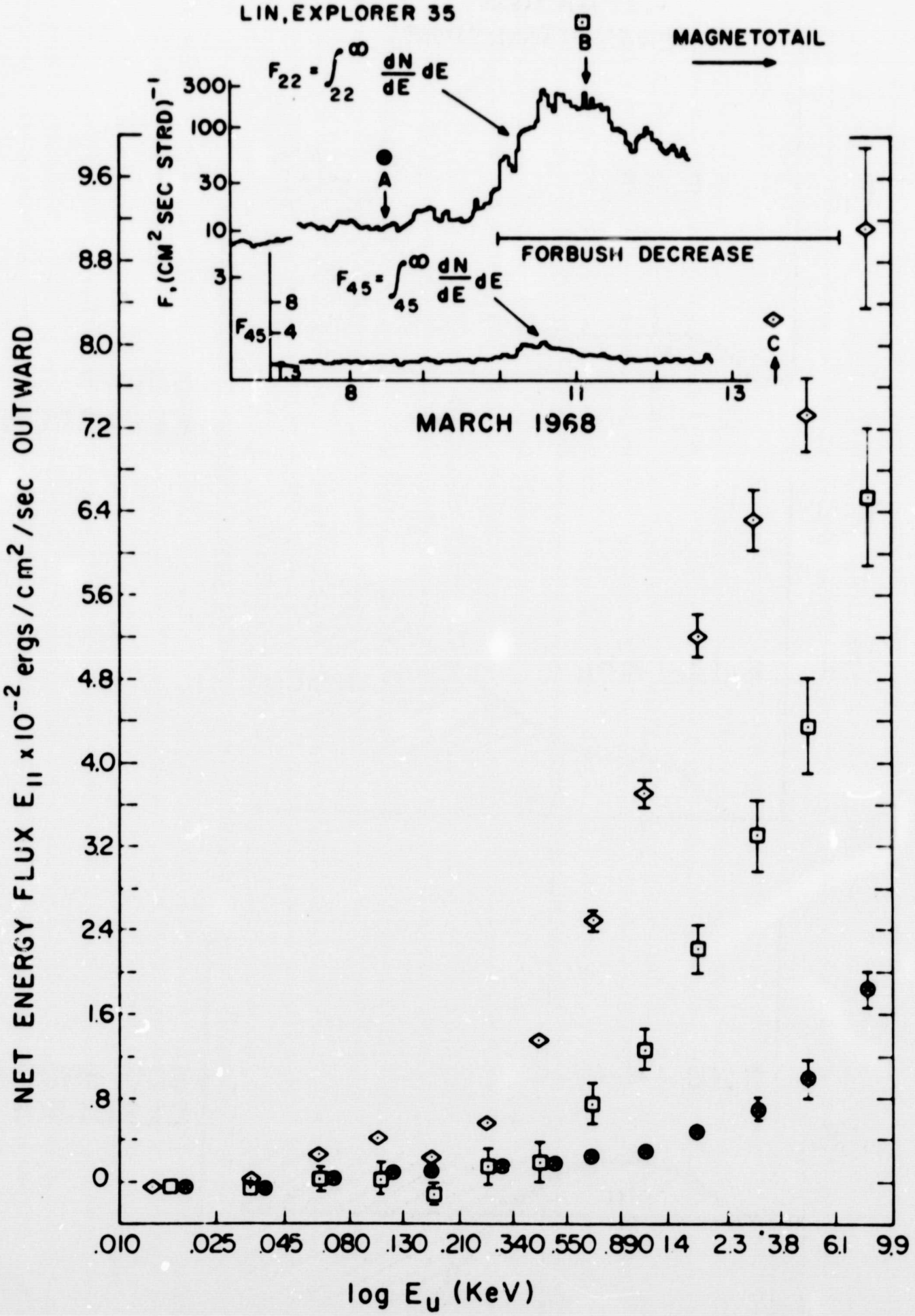
LIN, EXPLORER 35
MAGNETOTAIL
B
A
C
$F_{22} = \int_{22}^{\infty} \frac{dN}{dE} dE$
$F_{45} = \int_{45}^{\infty} \frac{dN}{dE} dE$
FORBUSH DECREASE
$F, (CM^2 SEC STRD)^{-1}$
300
100
30
10
3
8
4
F_{45}
8
11
13
MARCH 1968
NET ENERGY FLUX $E_{11} \times 10^{-2}$ ergs/cm^2/sec OUTWARD
9.6
8.8
8.0
7.2
6.4
5.6
4.8
4.0
3.2
2.4
1.6
.8
0
.010
.025
.045
.080
.130
.210
.340
.550
.890
1.4
2.3
3.8
6.1
9.9
log E_u (KeV)

Figure 6

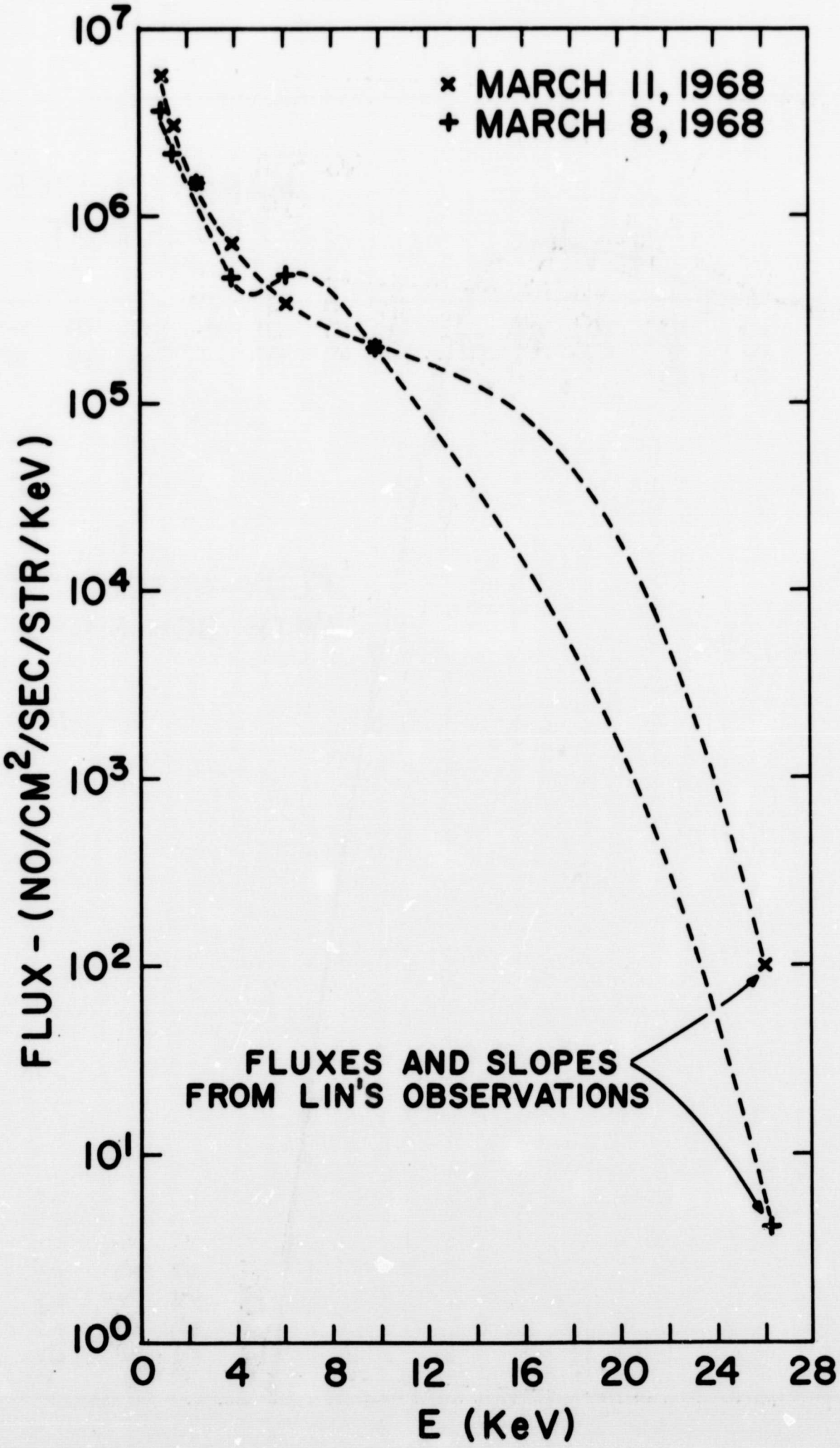
× MARCH 11, 1968
+ MARCH 8, 1968
FLUXES AND SLOPES
FROM LIN'S OBSERVATIONS
FLUX - (NO/CM²/SEC/STR/KeV)
E (KeV)
10⁷
10⁶
10⁵
10⁴
10³
10²
10¹
10⁰
0
4
8
12
16
20
24
28

Figure 7

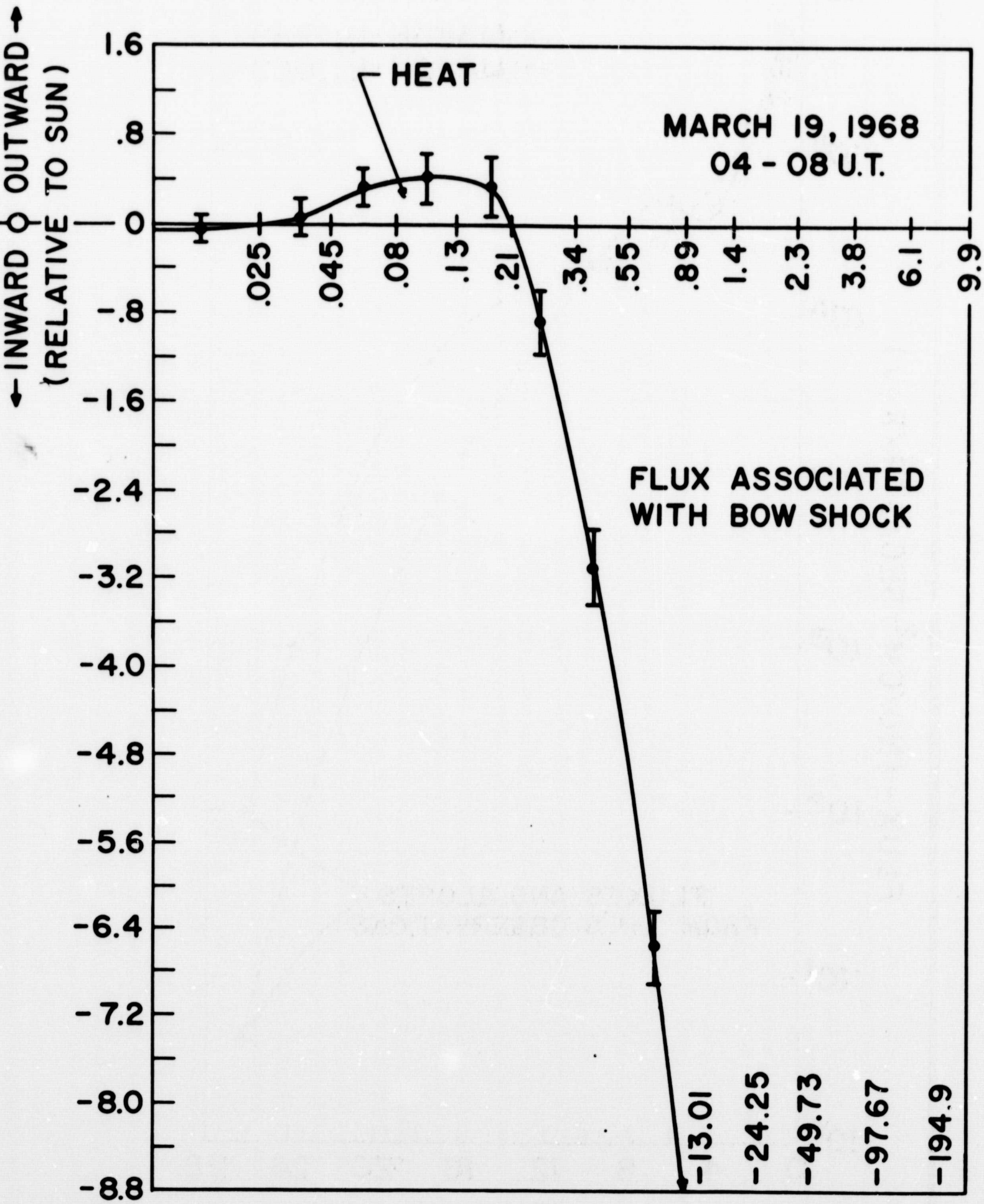
← INWARD ○ OUTWARD →
(RELATIVE TO SUN)
1.6
.8
0
-.8
-1.6
-2.4
-3.2
-4.0
-4.8
-5.6
-6.4
-7.2
-8.0
-8.8
HEAT
MARCH 19, 1968
04 - 08 U.T.
FLUX ASSOCIATED
WITH BOW SHOCK
.025
.045
.08
.13
.21
.34
.55
.89
1.4
2.3
3.8
6.1
9.9
-13.01
-24.25
-49.73
-97.67
-194.9

Figure 8